

# Non-Destructive Characterization of Hollow Core Fiber

Leonard Budd,<sup>1,\*</sup> Austin Taranta,<sup>1</sup> Eric Numkam Fokoua,<sup>1</sup> and Francesco Poletti<sup>1</sup>

<sup>1</sup> Optoelectronics Research Centre, University of Southampton, University Rd, Southampton SO17 1BJ, UK

\*l.g.budd@soton.ac.uk

**Abstract:** We summarize our recent work developing a technique for accurate and non-destructive measurement of the microstructure geometry of nested and double nested antiresonant fibers. We present results showing microstructure variation along a 2.2 km fiber.

© 2024 The Author(s)

## 1. Introduction

Guiding light in air or vacuum has long been an enticing prospect to researchers as they seek new technologies to overcome the penalizing intrinsic limits of conventional solid core silica fibers, such as loss from Rayleigh scattering in the bulk material and signal degradation due to optical non-linearity. Hollow core fibers (HCFs) guide light through a central hollow core, where it is confined through interactions with a surrounding cladding microstructure. Despite the first practical demonstration of an HCF coming almost 25 years ago [1], it was not until the relatively recent advent of so-called ‘antiresonant’ fiber (ARF) designs that these fibers demonstrated the required properties to be considered potentially viable for telecommunication applications. ARF microstructure is characterized by a series of thin glass membranes surrounding the core and light is confined to the core through antiresonant reflections with these membranes; that is, at certain antiresonant wavelengths, light will experience high reflectance from the membranes and hence be strongly confined.

In particular, two such microstructure geometries, the nested and double-nested antiresonant nodeless fiber (the NANF [2] and DNANF [3] respectively), have proved highly promising and have demonstrated the lowest loss in any HCF at 1550 nm (0.174 dB/km for a DNANF design). These fibers have a microstructure consisting of multiple circular glass capillaries spaced evenly around the core. Each capillary contains a smaller, nested capillary (one in the case of NANF, two in the case of DNANF) which provides an additional antiresonant reflecting layer which confines light more strongly to the core and further reduces the propagation loss of the fiber. To achieve the exciting potential properties of these fibers, precise control of the delicate glass microstructure is required at all points along the fiber’s length. One of the key challenges which must be overcome to improve the reliability of the fabrication process is the development of a method for non-destructively measuring this microstructure geometry whilst the fiber is being drawn. Currently, the microstructure is measured by cutting a small sample of the fiber mid-draw, viewing it under a microscope and making adjustments to the draw parameters to obtain the desired structure. This method greatly reduces the yield of fiber which can be drawn from a given preform and leads to the possibility of defects between sample points going unnoticed post-draw characterization. A method for non-destructive real-time microstructure characterization is hence highly desirable. Such a method is analogous to the non-contact laser gauges used to provide continuous feedback during draws of conventional silica fiber. An equivalent method for NANF and DNANF would help improve the reliability of fiber draws, increasing yield, reducing fabrication costs and potentially even leading to full automation of the draw process. Here we present results from our ongoing work developing a non-destructive side-scattering method to accurately measure the capillary diameters in NANF and DNANF. We provide an overview of the operating principles of this technique, show results from non-destructive measurements of small samples of NANF and DNANF and finally present non-destructive capillary diameter measurements along a 2.2 km sample of NANF.

## 2. Non-Destructive Hollow Core Fiber Measurement

A variety of methods for non-destructively characterizing the inner geometry of some HCFs and other microstructured fibers have been reported in the literature. These include optical tomography methods for reconstructing the refractive index profile of photonic crystal fibers [4–6], X-ray tomography for accurate characterization of hollow-core photonic crystal fibers and their preforms [7], and a side-scattering method used to measure the inner diameter of a capillary HCF based on its diffraction pattern [8].

The non-destructive measurement technique presented here was first described in 2019 for tubular ARFs (a cladding microstructure consisting of a single ring of glass capillaries with no nested elements) [9]. Here it was shown that by shining light on the side of an HCF and picking off a portion of the scattered light, inferences about the microstructure geometry could be made by analyzing the resulting interference pattern. A schematic of the setup for this measurement technique and the various optical paths taken by the light around the fiber microstructure is shown in Figure 1. Light from a broadband white light source (spectrum in Figure 1a) coupled

into a multimode fiber MM1 is collimated by a lens L and passes through a polarizing beam splitter PBS, after which it is incident on the side of an HCF which proceeds to scatter the light, some of which is collected by the multimode fiber MM2 at some angle  $\theta$  from the incoming light. MM2 is connected to a spectrometer which operates using an integration time of 50 ms. In the HCF, a portion of the light reflects off the air-glass interface between the core and the cladding (Figure 1c), taking an amount of time  $\tau_0$  to arrive at the collection fiber. Other fractions of this light make a single round trip of the outer (Figure 1d) and inner (Figure 1e) capillaries, taking additional time ( $\tau_1$  and  $\tau_2$  respectively) to arrive at the collection fiber. We see an interference pattern between these optical paths (Figure 1f), and an inverse Fourier transform to the time domain yields peaks corresponding to the time delay between the various paths (Figure 1g). Note the two peaks at  $\tau_1$  and  $\tau_2$ , as well as the additional spurious peak at  $\tau_1 - \tau_2$ . In [10], we showed that this spurious difference signal could be minimized through careful adjustment of the collection angle  $\theta$ . A simple geometrical model of the optical paths around the fiber microstructure can be used to map the temporal positions of the interference peaks to accurate measurements of the various capillary diameters [10, 11].

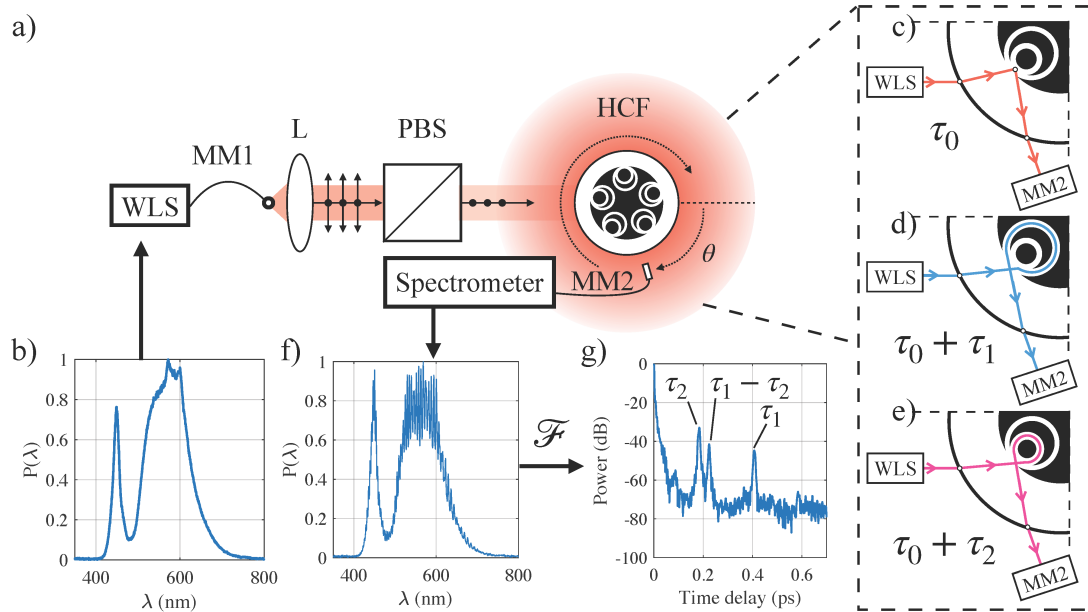


Fig. 1. Non-destructive measurement system. Setup (a), source spectrum (b), optical paths around microstructure (c-e), example scattering spectra (f) and time delay trace (g). Figure from [10]

### 3. Measurement of NANF and DNANF Microstructure

Here we show non-destructive measurements of NANF and DNANF microstructures, as originally presented in [12, 13]. Both fiber samples were held in place between two motorized rotation stages, allowing the fiber to be rotated fully and all 5 nested capillary diameters to be measured accurately at one point along the length of the fiber. The results of these measurements are shown in Figure 2. A cross-section of the NANF sample we used for this experiment is shown in Figure 2a. This fiber has a mean outer capillary diameter  $d_1$  of 26.6  $\mu\text{m}$  and a mean inner capillary diameter  $d_2$  of 12.1  $\mu\text{m}$ . Non-destructive and microscope measurements of the 5 inner and outer capillary diameters are shown in Figure 2b (blue circles and red crosses respectively). From this, we can see that there is excellent agreement between the two measurement methods (0.7% and 1.2% mean discrepancy for the inner and outer capillaries respectively), and the non-destructive measurement technique is able to capture the

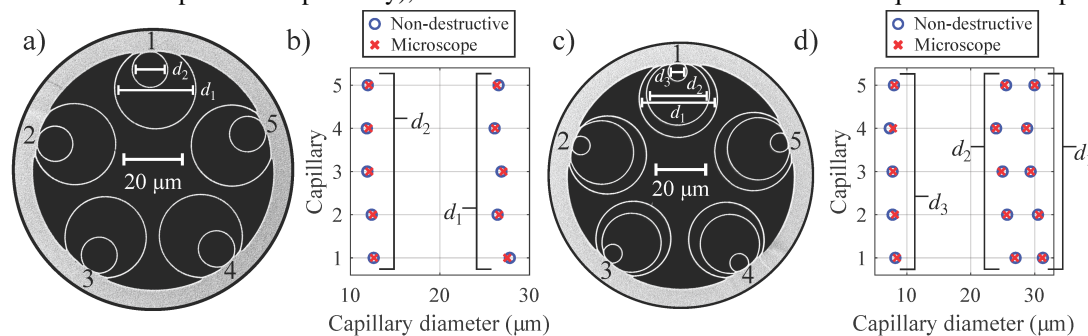


Fig. 2. Non-destructive measurement of NANF (fiber cross section in (a) and results in (b)) and DNANF (fiber cross section in (c) and results in (d)). Figure adapted from [10].

sub-micron variation in diameter between the various elements. Similarly for DNANF, we can accurately measure the three nested capillary diameters. The fiber sample (cross-section in Figure 2c) has mean outer, middle and inner capillary diameters of  $d_1=29.9\ \mu\text{m}$ ,  $d_2=25.4\ \mu\text{m}$  and  $d_3=8.0\ \mu\text{m}$  respectively. As before, there is excellent agreement between the two measurement methods, with mean discrepancies of 0.3%, 0.6% and 3% for the outer, middle and inner capillaries respectively. Note that, as described in [10], a correction for the inset of the small inner capillary into the surrounding glass jacket tube has been applied to increase the accuracy of the measurement.

#### 4. Longitudinal Measurement of NANF Microstructure Geometry

We can also non-destructively measure how the microstructure varies along the length of a fiber [14]. Here, the light source and spectrometer system was placed in the path of a fiber re-winder, and 2.2 km NANF was passed through it. Measurements of the mean inner and outer capillary diameter along the sample are shown in Figure 3a and b respectively. A microscope image of the fiber cross-section is shown in Figure 3. The fiber was run through the re-winder 3 times; twice at a speed of 4 m/min (red and blue traces, with blue trace reversed), and at 36 m/min (green trace) to demonstrate measurement at speeds comparable to a fiber draw. From the microscope measurements at either end of the sample (black crosses on the capillary diameter plots), there appears to be little variation in the fiber microstructure along its length (a 2.1% and 0.5% change in inner and outer diameters respectively). However, in all 3 non-destructive measurement traces, we see that there is in fact considerable variation (an increase of up to  $1\ \mu\text{m}$ ) in both inner and outer capillary diameter at both 0.9 and 1.3 km along the length. This corresponds to an increase of 6.4% for the inner capillaries, and 4.4% for the outer capillaries, likely indicating a change in fabrication parameters at these points. That we can capture such variation in rapidly moving fiber makes this method a potentially suitable candidate for real-time inline monitoring of fiber microstructure during fabrication.

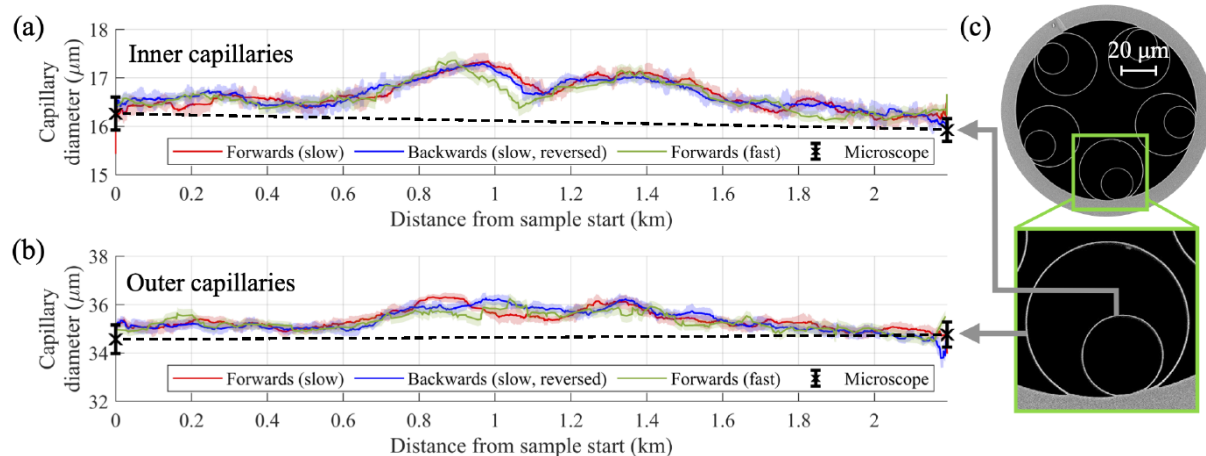


Fig. 3. Non-destructive measurement of mean inner (a) and outer (b) capillary diameter along a 2.2 km sample of NANF (cross-section in (c)). Figure from [14].

#### 5. Conclusions

To facilitate the mass-production of long lengths of NANF and DNANF, a method for non-destructively characterizing their microstructure during fabrication will most likely be necessary. Here we have provided an overview of such a technique, describing the underlying principles, showing accurate measurement of all capillary elements in small NANF and DNANF samples, and finally demonstrating non-destructive measurements of capillary diameter variation along 2.2 km of NANF moving through the measurement system at speeds comparable to a fiber draw. The speed and accuracy of these non-destructive measurements strongly motivate this method as a candidate for real-time inline structural monitoring.

We acknowledge funding from ERC (Airguide Photonics, EP/P030181/1), UK RAEng, Honeywell Inc. and the U.S. Government under the DoD Ordnance Technology Consortium (DOTC) Other Transaction Agreement (OTA) (W15QKN-18-9-1008).

#### References

1. R. F. Cregan *et al.*, *Science* **285**, 1537 (1999).
2. F. Poletti, *Opt. Express* **22**, 23807 (2014).
3. G. T. Jasion *et al.*, in *OFC*, (2022), Th4C.7.
4. W. Gorski and W. Osten, *Opt. Lett.* **32**, 1977 (2007).
5. A. D. Yablon, *Opt. Lett.* **38**, 4393 (2013).
6. A. Stefani *et al.*, *Opt. Express* **22**, 25570 (2014).
7. S. R. Sandoghchi *et al.*, *Opt. Express* **22**, 26181 (2014).
8. S. Schmidt *et al.*, *Opt. Lett.* **42**, 4946 (2017).
9. M. H. Frosz *et al.*, *Opt. Express* **27**, 30842 (2019).
10. L. Budd *et al.*, *Opt. Express* **31**, 36928 (2023).
11. Y. Xiong *et al.*, *Opt. Express* **30**, 48061 (2022).
12. L. Budd *et al.*, in *IEEE IPC*, (2021), ThG2.2.
13. L. Budd *et al.*, in *OSA APC*, (2022), SoTh3G.1.
14. L. Budd *et al.*, in *OFC*, (2023), W4D.2.